American Mineralogist, Volume 69, pages 1025–1035, 1984

Experimentally determined stability of clinopyroxene + garnet + corundum in the system $CaO–MgO–Al_2O_3–SiO_2$

TIBOR GASPARIK

Department of the Geophysical Sciences
University of Chicago
Chicago, Illinois 60637

Abstract

In the system $CaO–MgO–Al_2O_3–SiO_2$, the equilibrium compositions of clinopyroxene and garnet coexisting with corundum were determined in 16 runs at 1300°C/19.5–31.6 kbar and 1500°C/29.8 kbar. The phase transition clinopyroxene → garnet ($CaTs_{50}Di_{46}En_4$ → $Gr_{64}Py_{36}$) was reversed at 1100°C/25.0 kbar and 1300°C/32.5 kbar. In the Mg-free system, the breakdown curve of calcium Tschermak pyroxene to grossular and corundum was reversed at 1300, 1400 and 1500°C and can be described by the expression: P(bar) = 55T(°C) − 53900. The data were modeled using the Redlich-Kister equation, providing the mixing properties of the diopside–calcium Tschermak pyroxene and the grossular–pyrope solid solutions. The resulting model indicates complex short-range order–disorder phenomena in both solid solutions. Activities of the Ca-Tschermak component in pyroxene are substantially lower than the mole fractions. A discontinuity in the mixing properties of pyrope-rich garnets, caused by ordering of Ca and Mg in the dodecahedral site, is implied. The model predicts unmixing at 828°C/1 bar and 870°C/20 kbar, with the crest of the solvus at $Gr_{70}Py_{30}$. A major disagreement was observed between the excess enthalpies of Gr–Py garnets predicted by the model and those calculated from the published heats of solution measurements. Calculated phase relations of the assemblage clinopyroxene + garnet + corundum and a T–X phase diagram for the join grossular–pyrope at 30 kbar are presented.

Introduction

Phase relations among minerals in the upper mantle can be approximated in the system $CaO–MgO–Al_2O_3–SiO_2$ (CMAS). In this model system, the multicomponent clinopyroxene (Cpx) and garnet (Ga) phases found in upper mantle xenoliths, are represented by relatively simple solid solutions. The clinopyroxene solution can have up to four components, but only two of them, diopside (Di–$CaMgSi_2O_6$) and calcium Tschermak pyroxene (CaTs–$CaAl_2SiO_6$) occur stably and form a complete solid solution; the other two, enstatite (En–$Mg_2Si_2O_6$) and calcium Eskola component (CaEs–$Ca_{0.5}AlSi_2O_6$), can be present only in limited concentrations. The garnet solution has two components: grossular (Gr–$Ca_3Al_2Si_3O_{12}$) and pyrope (Py–$Mg_3Al_2Si_3O_{12}$). Thermobarometry based on phase relations in the CMAS system or in corresponding natural systems requires use of mixing properties of the clinopyroxene and the garnet solid solutions, which, until now, have been inadequately known. Equilibria in the assemblage clinopyroxene + garnet + corundum (Cor) provide an opportunity to study both garnet and pyroxene solutions and obtain additional constraints on their respective mixing properties.

The mixing properties of the Di–CaTs solid solution have been experimentally studied by Wood (1979) and Gasparik and Lindsley (1980), using phase equilibria in the assemblage clinopyroxene + anorthite (An) + quartz(Q). However, clinopyroxene in this assemblage contains a significant amount of Ca-Eskola component. Mixing properties of the Di–CaTs solution inferred from this silica-saturated ternary system are ambiguous, because they depend on the solution model used for extrapolation. In the assemblage Cpx + Ga + Cor, clinopyroxene is also a ternary solid solution, with endmembers diopside, Ca-Tschermak pyroxene and enstatite. However, the enstatite content of clinopyroxene, particularly in the CaTs-rich part of the solid solution, is very small, which reduces the uncertainty connected with extrapolation to the Di–CaTs join. Therefore, equilibria involving Cpx + Ga + Cor should provide more reliable constraints on the mixing properties of the Di–CaTs solution than the equilibria in the assemblage Cpx + An + Q.

There are few phase equilibrium data constraining mixing properties of the grossular–pyrope solid solution. Hensen et al. (1975) determined grossular activities in the Gr–Py garnets in the compositional range $Gr_{90}Py_{10}$–$Gr_{78}Py_{22}$. In contrast, phase equilibria involving the assemblage Cpx + Ga + Cor include stable garnets in the

0003–004X/84/1112–1025$02.00

range Gr_{100}–$Gr_{20}Py_{80}$.

Compositions of phases in the assemblage Cpx + Ga + Cor are limited to the ternary system $CaSiO_3$–$MgSiO_3$–Al_2O_3. Boyd (1970) determined phase relations in this system at 1200°C and 30 kbar (nominal) and found two stability fields of the assemblage Cpx + Ga + Cor as a result of instability of intermediate garnet compositions with respect to Cpx + Cor. At slightly higher pressure, Chinner et al. (1960) had reported complete garnet solution. Additional relevant data have been obtained by Malinovskii et al. (1976) and Maaløe and Wyllie (1979). Haselton and Newton (1980) attempted to model the phase relations of the assemblage Cpx + Ga + Cor, relying mainly on thermochemical data. They concluded that uncertainties in the thermochemical properties, particularly for the clinopyroxene solid solution, did not allow quantitative calculations of the phase relations.

Several major obstacles still exist in an attempt to calculate the phase relations of the assemblage Cpx + Ga + Cor: (1) The existing experimental data are inadequate because they are not reversed; (2) The thermodynamic properties of the clinopyroxene and the garnet solid solutions are not well-known. This paper presents phase equilibrium data needed to obtain better constraints on the mixing properties of both solid solutions, and to calculate the phase relations of the assemblage Cpx + Ga + Cor.

Phase relations involving Cpx + Ga + Cor have direct application in the thermobarometry of corundum eclogites and grospydites (Sobolev et al., 1968). Although mantle xenoliths more commonly contain kyanite (Ky) instead of corundum, the phase relations of the assemblage Cpx + Ga + Ky should be quite similar to the phase relations of the assemblage Cpx + Ga + Cor, and can be calculated using the results given below.

Experimental techniques

General procedures

Experiments were carried out using a conventional piston-cylinder apparatus with a ½″ diameter assembly made of talc and soft glass. Samples were encased in platinum capsules. Description of the assembly and experimental procedures are given by Gasparik and Newton (1984). For this assembly, the authors found a temperature-dependent pressure correction of $-[26.5 - 0.015T(°C)]\%$, based on calibration against the spinel peridotite–garnet peridotite boundary. The nominal pressure was kept within ±200 bars of the run value. Temperature was measured by W-3%Re vs. W-25%Re thermocouples and controlled automatically. No correction for the effect of pressure on emf was applied. The uncertainty in the temperature is less than ±5°C.

Starting materials

The starting materials were mechanical mixes made of ultrapure oxides and $CaAl_2O_4$ (Table 1). $CaAl_2O_4$ was prepared by sintering a mix of $CaCO_3$ and Al_2O_3 first at 700°C for 24 hours, and then at 1300°C for 24 hours. PbO was used in the starting materials as flux to promote equilibration of charges. Large crystals of synthetic diopside, Ca-Tschermak pyroxene, and garnet of several compositions were added to the starting materials in amounts of approximately 3 wt.% each.

Table 1. Compositions of starting materials (in moles)

	$CaAl_2O_4$	MgO	Al_2O_3	SiO_2	PbO
A	0.95	0.05	0.25	1.30	0.30
B	0.90	0.10	0.30	1.30	0.30
C	0.87	0.13	0.33	1.30	0.30
D	0.83	0.17	0.37	1.30	0.30
E	0.78	0.22	0.42	1.30	0.30
F	0.71	0.29	0.49	1.30	0.30
G	0.62	0.38	0.48	1.30	0.30
H	0.59	0.41	0.51	1.30	0.30
I	0.54	0.46	0.56	1.30	0.30
J	0.50	0.50	0.60	1.30	0.30
K	0.44	0.56	0.66	1.30	0.30
L	0.40	0.60	0.70	1.30	0.30
M	0.40	0.60	0.80	1.30	0.30
N	0.38	0.62	0.72	1.30	0.30
O	0.34	0.66	0.76	1.30	0.30
P	0.40	0.60	0.70	1.10	0.10
Q	0.67	0.33	0.43	1.30	0.30
R	1.00	-	-	1.00	0.03
S	1.10	-	-	1.00	-
T	0.66	0.34	0.44	1.08	0.08
U	0.32	0.68	0.48	1.05	0.05

All equilibration experiments produced the assemblage Cpx + Ga + Cor + PbO-rich liquid. The large pyroxene and garnet crystals equilibrated with coexisting phases approaching the equilibrium compositions from different directions. Thus, the equilibrium pyroxene compositions were approached from two directions by reequilibration of the diopside and the Ca-Tschermak seeds. Garnet seeds, however, in most cases dissolved if their compositional reequilibration paths entered regions in which they were metastable with respect to Cpx + Cor. Thus it was possible to reverse the garnet composition only in two experiments.

Analytical procedures

Experiments produced hard pellets composed of crystals surrounded by PbO-rich glass. Approximately half of a pellet was ground and used for verifying the presence of the assemblage Cpx + Ga + Cor by X-ray diffraction. The other half of the charge was mounted for microprobe analysis.

Energy dispersive microprobe analyses were obtained with an ARL-EMX electron microprobe. All analyses were made at 15 kV with a minimum spot size ($\approx 1\mu m$). Standards used were synthetic glasses covering a wide range of pyroxene and garnet compositions (Di_{100}, $Di_{80}CaTs_{20}$, $Di_{60}CaTs_{40}$, $Di_{40}CaTs_{60}$, $Di_{20}CaTs_{80}$, $En_{80}MgTs_{20}$, $Gr_{90}Py_{10}$, $Gr_{80}Py_{20}$). Analyses were obtained

Table 2. Conditions of equilibration experiments and average compositions of clinopyroxene and garnet coexisting with corundum and PbO-bearing liquid. Temperature is 1300°C, except for the run #749, T = 1500°C.

Run #	P[a] (kb)	t (hrs.)	Mix[b]	Seeds[c]	Px[d] an.	Cations/6 oxygens Ca	Mg	Al	Si	X^{Px}_{CaTs}	X^{Px}_{En}	Ga[d] an.	Cations/12 oxygens[e] Ca	Mg	Si	X^{Ga}_{Gr}
549	24	23.0	A	DCG	63	0.994	0.139	1.733	1.134	0.867	0.006	28	2.891	0.111	2.998	0.963
575	26	23.0	B	DCG	58	0.988	0.205	1.599	1.204	0.801	0.012	28	2.817	0.190	2.993	0.937
590	28	22.0	C	DCGP2	44	0.994	0.269	1.475	1.262	0.737	0.006	60	2.711	0.290	2.999	0.903
628	30	22.5	D	DCGP2	53	0.990	0.324	1.380	1.308	0.689	0.010	48	2.617	0.396	2.987	0.869
607	32	23.0	E	DCG	37	0.973	0.393	1.252	1.378	0.627	0.027	16	2.414	0.590	2.997	0.804
613	34	23.0	F	DCG	40	0.973	0.450	1.130	1.441	0.566	0.027	32	2.226	0.772	3.002	0.743
620	34	22.5	G	CP8	21	0.944	0.557	0.977	1.517	0.489	0.057	36	1.516	1.489	2.996	0.505
614	33	22.5	H	DCP8	30	0.920	0.601	0.938	1.536	0.470	0.081	21	1.353	1.654	2.992	0.450
612	32	23.0	I	CP8	23	0.940	0.611	0.880	1.565	0.440	0.061	37	1.306	1.702	2.992	0.434
602	31	23.0	J	DCP8	32	0.914	0.618	0.912	1.550	0.457	0.087	28	1.203	1.810	2.987	0.399
608	29	22.0	K	DP8	13	0.918	0.638	0.859	1.578	0.430	0.083	15	1.027	1.984	2.988	0.341
581	27	23.5	L	DP8	20	0.909	0.681	0.807	1.600	0.404	0.092	10	0.870	2.151	2.979	0.288
550	25	22.0	M	DCP	52	0.903	0.710	0.766	1.619	0.383	0.097	16	0.808	2.201	2.992	0.268
596	23	23.0	N	DCP8	53	0.893	0.718	0.772	1.616	0.386	0.107	15	0.722	2.293	2.984	0.240
584	21	22.0	O	DP8	42	0.860	0.776	0.724	1.640	0.362	0.140	14	0.612	2.412	2.976	0.203
749	31	6.0	P	DCP	44	0.889	0.654	0.926	1.535	0.463	0.111	20	0.781	2.235	2.983	0.259
618[f]	35	22.5	Q	GP8	-							67	1.894	1.117	2.989	0.629

a Nominal pressures; $P_{"real"} = [0.735 + 15x10^{-5}T(°C)]P_{nominal}$.
b Bulk compositions of mixes are given in Table 1.
c Seed crystals from which analyses were obtained: D=diopside; C=Ca-Tschermak pyroxene; G=grossular; P=pyrope; P2,P8=garnet of composition $Py_{20}Gr_{80}$ and $Py_{80}Gr_{20}$ respectively.
d The total number of pyroxene/garnet analyses accepted from a given run.
e The number of Al cations in the garnet analyses is not listed, because in most cases the Al counts were altered by small amounts of corundum included in the garnet. The sum of the remaining cations was set to 6.
f The run produced assemblage Ga+Cor+L with corroded relics of Di and CaTs seeds. The matrix did not contain pyroxene.

from reaction rims developed around the seed crystals. Original compositions were preserved in the cores of seeds; thus it was always possible to infer the direction of the approach to equilibrium. Typically about 20 analyses were taken from several grains of each kind of seed. In most experiments, compositional fields obtained from both kinds of pyroxene seeds completely overlapped indicating that equilibrium was closely approached. Lead content of all crystalline phases was below the detection limit.

Experimental results

Equilibrium compositions of clinopyroxene and garnet coexisting with corundum were obtained at 16 different P–T conditions (Table 2). All equilibration experiments were at 1300°C with the exception of the run #749 which was at 1500°C. For each experiment, an average composition for equilibrated rims on each kind of seed was calculated separately. The resulting averages obtained from the diopside and the Ca-Tschermak seeds were then averaged to give the equilibrium composition used in the least squares solution modeling and listed in Table 2. Mole fractions of pyroxene components were calculated from cations per 6 oxygens using the following expressions:

$$X_{En} = 1 - Ca;$$

$$X_{CaTs} = (2 - Si + 0.5Al)/2;$$

$$X_{Di} = (Mg - 2X_{En} + Ca - X_{CaTs})/2.$$

The sum of the mole fractions was then normalized to one.

The 1300°C experimental results are shown in Figure 1. The data indicate two stability fields of Cpx + Ga + Cor joined at the crest of the solvus where clinopyroxene transforms directly to garnet. This transition was reversed at 1300°C and 32.7±0.3 kbar, and at 1100°C and 25.0±0.25 kbar (Table 3). The reaction was first located by synthesis experiments, products of which were used to prepare the reversal mix. Because the reaction did not go to completion, it was necessary to establish that the bulk composition used for the reversals produced clinopyroxene and garnet with compositions on the crest of the solvus. The bulk composition used for the reversals at 1300°C was also used in the synthesis experiment #618 at 1300°C/32.6 kbar (Table 2), which contained seeds of Di, CaTs, Gr, and $Gr_{20}Py_{80}$. Experimental product was Ga + Cor + L with relics of the pyroxene seeds. The matrix, however, did not contain any pyroxene. Microprobe analyses indicate an average garnet composition $Gr_{63}Py_{37}$, very close to the composition inferred for the crest of the solvus. In the experiment #709 (Table 3), which represents the high-pressure bracket at 1100°C, the garnet composition $Gr_{67}Py_{33}$ was determined by slow scan X-ray diffraction using the calibration of Newton et al. (1977).

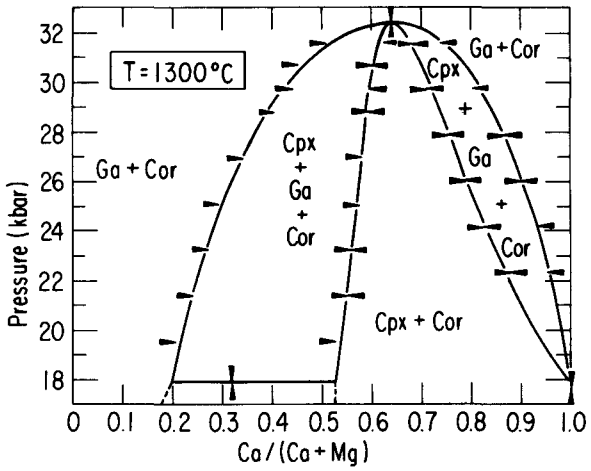

Fig. 1. *P–X* phase relations of the assemblage Cpx + Ga + Cor at 1300°C, with the composition expressed as atom ratio of Ca/(Ca + Mg). The present data are indicated by the tip of the arrows pointing in the direction of the approach to equilibrium. Shown also is the calculated fit to the data. For the Mg-rich bulk compositions, the stability of the assemblage Cpx + Ga + Cor is limited by reaction to Sp + An.

Additional experimental data locating the limits of stability for Cpx + Ga + Cor are also given in Table 3. In the Mg-free system, the breakdown curve of CaTs to Gr + Cor was reversed at 1300, 1400, and 1500°C. A reversal mix with approximately equal amounts of reactants and products was prepared from crystalline material synthesized with the piston-cylinder apparatus using ¾″ talc-pyrex assembly and graphite sample containers. Ca-Tschermak pyroxene was synthesized at 1400°C/20 kbar (nominal) and Gr + Cor at 1300°C/26 kbar, from the same mix.

Table 3. Experimental runs on univariant reactions (R.): 3CaTs = Gr + 2Cor (1), Cpx = Ga (2), and Cpx + Ga + Cor = Sp + An (3). Starting materials were reversal mixes with approximately equal amounts of reactants and products. Capital letters in parentheses in the table refer to the compositions of starting materials listed in Table 1.

R.	Run #	T (°C)	P* (kbar)	t (hrs.)	Starting material	Result
1	600	1300	18.5	23.0	CaTs+Gr+Cor (R)	CaTs
1	597	1300	19.0	23.5	CaTs+Gr+Cor (R)	Weak growth of Gr+Cor
1	735	1400	24.0	23.0	CaTs+Gr+Cor (S)	Strong growth of CaTs
1	734	1400	24.6	23.0	CaTs+Gr+Cor (S)	Gr+Cor
1	727	1500	29.7	6.0	CaTs+Gr+Cor (S)	Strong growth of CaTs
1	723	1500	30.0	6.0	CaTs+Gr+Cor (S)	Strong growth of Gr+Cor
2	712	1100	27.5	22.5	Cpx+Ga+Cor (T)	Cpx grew
2	709	1100	28.0	26.0	Cpx+Ga+Cor (T)	Ga grew
2	630	1300	34.8	23.0	Cpx+Ga+Cor (Q)	Cpx grew
2	634	1300	35.5	22.5	Cpx+Ga+Cor (Q)	Ga grew
3	759	1300	19.0	23.0	Cpx+Ga+Cor+Sp+An (U)	Sp+An grew
3	754	1300	19.5	23.0	Cpx+Ga+Cor+Sp+An (U)	Ga+Cor+(Cpx) grew

* Nominal pressures: $P_{\text{"real"}} = [0.735 + 15\times10^{-5}T(°C)]P_{\text{nominal}}$.

In the Mg-rich part of the CMAS system, the stability of the assemblage Cpx + Ga + Cor is terminated by reaction to spinel + anorthite. This reaction was reversed at 1300°C and 17.9 ± 0.25 kbar (Table 3). The reversal mix was prepared from the products of synthesis experiments obtained at 1300°C and 19.5 or 20.5 kbar (nominal). The synthesis experiments were seeded with garnet of composition $Gr_{15}Py_{85}$.

Thermodynamic evaluation of results

Equilibrium in the assemblage Cpx + Ga + Cor is controlled by three endmember reactions,

$$3CaTs^{Cpx} = Gr^{Ga} + 2Cor; \quad (1)$$

$$3En^{Cpx} + 2Cor = 2Py^{Ga}; \quad (2)$$

$$3Di^{Cpx} + 2Cor = Gr^{Ga} + Py^{Ga}. \quad (3)$$

Equilibrium condition for the reactions has been expressed as:

$$RT\ln K_{eq} + \Delta G^{\circ}_{T,P} = 0$$

and the standard free energy change of an equilibrium was evaluated by choosing the reference temperature at 970 K:

$$\Delta G^{\circ}_{T,P} = \Delta H^{\circ}_{970,1} - T\Delta S^{\circ}_{970,1} - \int_{970}^{T}\int_{970}^{T} \Delta C_P/T\, dT dT + \int_{1}^{P} \Delta V^{\circ}_{T,P} dP,$$

where

$$\int_{1}^{P} \Delta V^{\circ}_{T,P}\, dP = [\Delta V^{\circ}_{298,1} + \Delta(\alpha V^{\circ})(T - 298) - 1/2\Delta(\beta V^{\circ})P]P.$$

Volume differences for all reactions were calculated using the unit cell volumes and the coefficients of isobaric thermoexpansion (α) and isothermal compressibility (β) from Table 4.

Reaction (1) can be described by expression: P(bar) = $55T$(°C) − 53900, based on data in Table 3. The standard free energy change of reaction (1) is (J, bar, K):

$$\Delta G^{\circ}(1) = -99300 + 79.8T - [1.43 + 8.7\times10^{-5}(T - 298) - 29\times10^{-7}P]P,$$

and the equilibrium condition for reaction (1) corresponds to:

$$3RT\ln(a_{Gr}/a_{CaTs}) + \Delta G^{\circ}(1) = 0,$$

where $a_{Gr} = X_{Gr} \cdot \gamma_{Gr}$, etc.

The location of the metastable reaction (2) can be obtained indirectly. Gasparik and Newton (1984) reported a reversal of the reaction

$$3En^{Opx} + 2Cor = 2Py \quad (4)$$

Table 4. Thermodynamic parameters used in this study

Mineral	$H^\circ_{f,970}$ (kJ/mol)	S°_{298} (J/mol.K)	C_p(J/mol.K) = a + bT + cT^{-2} + $dT^{-0.5}$ + eT^2 a	b x 10^3	c	d	e x 10^5	$V^\circ_{298,1}$ (J/bar)	α x 10^5	β x 10^7
Diopside	-146.4[a]	143.09[e]	328.19[i]	1.888	-1443000	-2519.2	0	6.613[j]	3.33[m]	8.2[q]
CaTs	-77.0[b]	135.30[f]	465.18[f]	-78.375	672940	-4921.1	1.9341	6.356[j]	2.90[n]	8.2[q]
Enstatite	-70.7[c]	132.54[g]	377.51[h]	-10.663	865	-3625.7	0	6.264[k]	3.20[o]	8.7[r]
Grossular	-326.0[a]	260.12[h]	516.33[h]	32.184	-9941900	-1403.1	0	12.523[l]	2.66[p]	6.4[p]
Pyrope	-84.6[d]	266.27[h]	544.95[h]	20.680	-8331200	-2283.0	0	11.320[l]	2.66[p]	6.4[p]
Corundum		50.92[e]	157.36[e]	0.719	-1896900	-988.0	0	2.558[e]	2.60[o]	3.6[s]

[a] Charlu et al. (1978); [b] Charlu et al. (1978), modified; [c] Gasparik and Newton (1984); [d] Charlu et al. (1975); [e] Robie et al. (1978); [f] Haselton et al. (1982); [g] Krupka et al. (1979); [h] Haselton (1979); [i] Holland (1981); [j] Gasparik (1981); [k] Chatterjee and Schreyer (1972); [l] Newton et al. (1977); [m] Cameron and Papike (1980); [n] This study; [o] Skinner (1966); [p] Hazen and Finger (1978); [q] Levien and Prewitt (1981); [r] Ralph and Ghose (1980); [s] Birch (1966).

in the system MgO–Al_2O_3–SiO_2 at 850°C/16.25 kbar. At these P–T conditions orthopyroxene contains 10.2 mole% of the MgTs component ($MgAl_2SiO_6$). The equilibrium condition can be expressed as (Gasparik and Newton, 1984):

$$-3RT\ln X_{En}^{Opx} + \Delta G^\circ(4) = 0, \text{ where}$$

$$\Delta G^\circ(4) = 72200 - 202.30T + 38T^{1.2} - [1.268 + 13.2 \times 10^{-5}(T - 298) - 19 \times 10^{-7}P]P.$$

By combining this expression with the transition

$$En^{Opx} = En^{Cpx}, \quad (5)$$

for which Lindsley *et al.* (1981) give

$$\Delta G^\circ(5) = 3560 - 1.91T - 0.0355P,$$

the standard free energy change of equilibrium (2) is obtained:

$$\Delta G^\circ(2) = \Delta G^\circ(4) - 3\Delta G^\circ(5)$$
$$= 61500 - 196.57T + 38T^{1.2} - [1.16 + 13.2 \times 10^{-5}(T - 298) - 19 \times 10^{-7}P]P.$$

The equilibrium condition for reaction (2) can be written as:

$$3RT\ln(a_{Py}^2/a_{En}) + \Delta G^\circ(2) = 0.$$

For the metastable reaction (3) the equilibrium condition is:

$$3RT\ln(a_{Gr} \cdot a_{Py}/a_{Di}) + \Delta G^\circ(3) = 0.$$

The standard free energy change of reaction (3) was determined by solution modeling of the experimental data, as described below, with the result:

$$\Delta G^\circ(3) = -5130 - 41.0T + 18T^{1.2} - [1.11 + 15.9 \times 10^{-5}(T - 298) - 14 \times 10^{-7}P]P.$$

The mixing properties of the pyroxene and the garnet solid solutions were modeled applying the Redlich–Kister equation (Redlich and Kister, 1948), because it was found necessary to use 3 fitting parameters for each of the Di–CaTs and the Gr–Py binaries in order to satisfy the data. Expressions for excess chemical potentials of all three components in a ternary solid solution are given in the Appendix.

Excess enthalpies of the Di–CaTs solid solution were based on the heats of solution measurements of Newton et al. (1977). Properties of the Di–En binary were taken from Lindsley et al. (1981). Excess volumes for the Di–CaTs and the Gr–Py solutions were calculated from the unit cell volume measurements of Gasparik (1981) and Newton et al. (1977) respectively. The quadratic-Gaussian approximation of the excess volume used by Haselton and Newton (1980) for the Gr–Py garnets has not been adopted, because it is not consistent with the solution model used in this study and would complicate extrapolation of the Gr–Py mixing properties to more complex garnet solutions.

The solution modeling procedure applied in this study is similar to the procedure used by Lindsley et al. (1981, p. 165–166). The input phase compositions are manually adjusted within reasonable limits allowed by the data until the residuals are reduced to insignificantly small values. After a number of cycles, a set of parameters is found that satisfies all data. This procedure, however, does not provide statistical information on the quality of the fit.

The data set used in the solution modeling consisted of 16 compositions of pyroxene and garnet in equilibrium with corundum (Table 2) and 2 reversals of the crest of the solvus (Table 3). The data, however, did not constrain well the mixing properties of the Di-rich part of the Di–CaTs solid solution, because the pyroxene compositions were limited to the range $CaTs_{100}$–$Di_{60}CaTs_{40}$. In order to obtain better constraints on the Di-rich part of the solid solution, the results from experiments with the assemblage Cpx + An + Q (Gasparik, 1981) were fitted simultaneously. Thus, it was possible to obtain excess parame-

ters for the Di–CaTs solid solution which satisfy both sets of data.

The least squares solution modeling of the present data resulted in the following expressions for the excess free energy of the Di–CaTs solid solution (G^{xs}_{Px}) and the Gr–Py solid solution (G^{xs}_{Ga}):

$$G^{xs}_{Px} = X_C X_D[10000 - 10T - 0.07P - (50000 - 31.19T + 0.04P)(X_C - X_D) - 7000(X_C - X_D)^2] + X_C X_E[14530 - 1.22T - 33810(X_C - X_E)] + X_D X_E[28350 + 0.038P - (2870 - 0.044P)(X_D - X_E)];$$

$$G^{xs}_{Ga} = X_G X_P[24660 - 13.91T + 0.16P + (39890 - 27.14T)(X_G - X_P) - 0.06P(X_G - X_P)^2],$$

where $X_{C,D,E,G,P,}$ = mole fractions of CaTs, Di, En, Gr, and Py in corresponding phases.

Discussion

The parameters obtained by solution modeling were used to calculate phase relations of the assemblage Cpx + Ga + Cor by simultaneously minimizing the free energy of all three endmember reactions. Figure 1 shows the quality of the fit of the model to the experimental data at 1300°C.

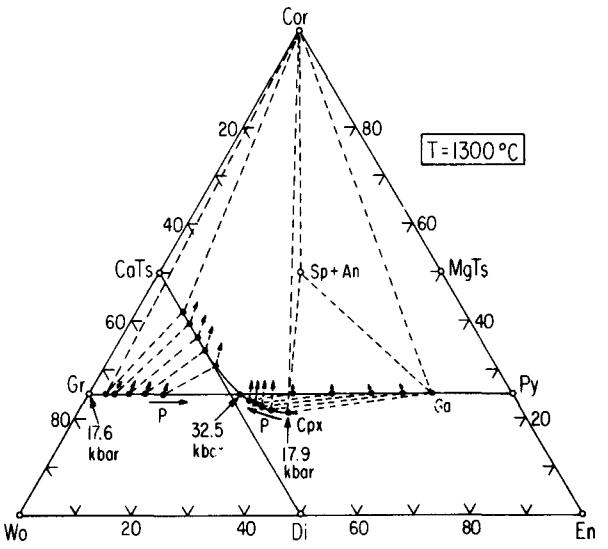

Fig. 2. Phase relations of the assemblage Cpx + Ga + Cor at 1300°C projected on the compositional plane $CaSiO_3$–$MgSiO_3$–Al_2O_3 (in mole percent). Explanation in the text.

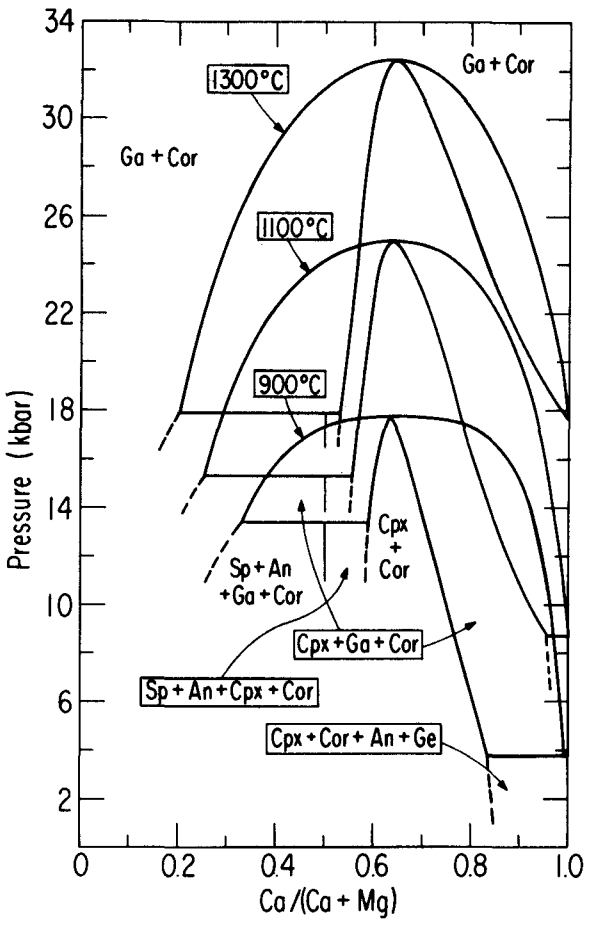

Fig. 3. Calculated *P–X* phase relations of the assemblage Cpx + Ga + Cor at 900, 1100 and 1300°C, with the composition expressed as atom ratio of Ca/(Ca + Mg).

In Figure 1 the clinopyroxene and garnet compositions are expressed in their Ca/(Ca + Mg) ratios. For the pyroxene, which is a ternary solution, this represents a simplification. For rigorous description of compositional relations, the three component triangle $CaSiO_3$–$MgSiO_3$–Al_2O_3 is more appropriate (Fig. 2). Compositions of clinopyroxene and garnet in equilibrium with corundum at 1300°C and various pressures are shown as solid dots connected by dashed lines. With increasing pressure, clinopyroxene and garnet compositions converge, approaching the same composition at 32.5 kbar, where clinopyroxene of composition $CaTs_{0.5}Di_{0.461}En_{0.039}$ transforms directly into garnet of composition $Gr_{0.641}Py_{0.359}$.

The phase relations determined at 1300°C have been extended to other temperatures with a few additional experiments. These consist of one equilibration run with the assemblage Cpx + Ga + Cor at 1500°C and 29.8 kbar (Table 2) and a reversal of the crest of the solvus at 1100°C and 25 kbar (Table 3). Figure 3 shows the phase

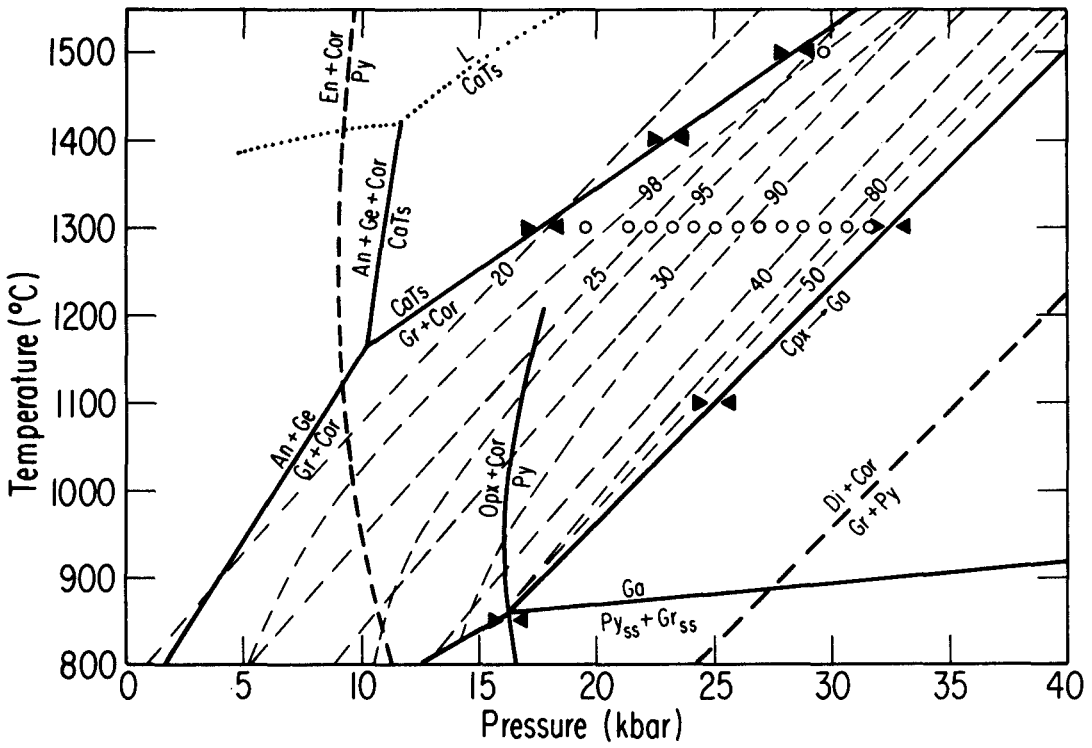

Fig. 4. *P–T* projection showing selected univariant equilibria (stable: thick solid lines; metastable: thick dashed lines) and calculated isopleths of mole percent of grossular in garnet in equilibrium with clinopyroxene and corundum (thin dashed lines). Shown also are reversals of the univariant equilibria (triangles) and the locations of equilibration experiments with the assemblage Cpx + Ga + Cor (open circles).

relations in a *P–X* projection calculated at 900, 1100, and 1300°C. At lower temperatures CaTs endmember is no longer stable and the Cpx + Ga + Cor field is terminated by the reaction

$$\text{Ga} + \text{Cor} = \text{Cpx} + \text{An} + \text{Ge (gehlenite)}. \quad (6)$$

The same phase relations are shown in a *P–T* projection in Figure 4. Shown also are important univariant curves and locations of all equilibration experiments and reversals of the univariant curves. The diagram is useful for comparing the model phase relations with some of the previous experimental results.

Chinner et al. (1960) report a complete solution between pyrope and grossular at 1250°C and 30 kbar corrected pressure. If the temperature effect on the pressure correction, not considered by the authors, is included, the experimental conditions would correspond to the crest of the present model solvus.

Based on synthesis experiments, Boyd (1970) gives compositions of clinopyroxene and garnet coexisting with corundum at 1200°C and 30 kbar nominal pressure (27.9 kbar corrected). This is 0.9 kbar below the crest of the solvus, where the reported compositions are in reasonable agreement with the present results.

The model reproduces most of the observed phase relations fairly well. The largest discrepancy between the observed and the calculated compositions is the clinopyroxene composition at 1500°C/29.8 kbar. The model predicts $X_{\text{CaTs}} = 0.40$ while the average measured CaTs content is 0.46 with the spread 0.43–0.50.

Other discrepancies are evident when comparing the obtained parameters with measured thermochemical data. A serious discrepancy is in the *P–T* location of reaction (3), for which the model gives:

$$\Delta G°(3) = -5130 - 41.0T + 18T^{1.2} + \int_1^P \Delta V°_{T,P}\,dP,$$

where

$$\int_{970}^{T}\int_{970}^{T} \Delta C_P/T\,dT\,dT = -13818 + 85.47T - 18T^{1.2}.$$

This gives $\Delta H°_{970,1} = -19.0$ kJ/mol and $\Delta S°_{970,1} = -44.5$ J/mol · K. In contrast, the thermochemical data from Table 4 predict $\Delta H°_{970,1} = 28.6$ kJ/mol and $\Delta S°_{970,1} = -4.7$ J/mol · K. It is difficult to point out exactly the reason for

such a discrepancy. The model itself is a relatively simple mathematical approximation of what could be very complex mixing properties of both solid solutions. Small differences between the predicted and the real mixing properties of the solid solutions could result in substantial discrepancies when extrapolated to endmembers. For example, it is possible to explain at least part of the discrepancy in $\Delta S°(3)$ if there were substantial disorder of calcium between the M2 and the M1 site in the pyroxene. Complete disorder would reduce the discrepancy by $3R\ln 2 = 17.3$ J/mol · K.

Another possibility is that the partial molar entropy of pyrope in the garnet solution is smaller than that predicted by the Third Law entropy of pyrope. This decrease in the entropy of pyrope should occur in the compositional range Py_{100}–$Gr_{20}Py_{80}$ which is not covered by the present experiments. The Third Law entropy of pyrope, 266.27 J/mol · K (Haselton, 1979), is anomalously high when compared with the entropy predicted by empirical entropy-volume relations for silicates. For example, Saxena (1976) gives the relation $S = 43.367V - 97.54n$ (n = 3) from which the entropy of pyrope should be 198.22 J/mol · K. The difference from the measured entropy is 68 J/mol · K, more than enough to account for the discrepancy is $\Delta S°(3)$. Newton et al. (1977) suggest that the anomalously high entropy of pyrope is the result of positional disorder of Mg in the dodecahedral site. This postulated positional disorder could possibly be reduced by adding 20% or less of calcium.

The final adopted mixing properties of both solid solutions represent a compromise achieved by fitting the heats of solution measurements on Di–CaTs pyroxenes (Newton et al., 1977) as shown in Figure 5. While it was possible to satisfy all measurements in the Di-rich half of the solid solution, the model required negative excess enthalpies in the CaTs-rich half of the solution, in contrast to a positive excess enthalpy measured for $Di_{30}CaTs_{70}$. Because the negative excess entropies predict substantial ordering in this compositional range, it is possible that the measurement reflects metastable disorder in the synthetic material obtained by devitrification of glass.

Model excess entropies predict large disorder in the Di-rich part of the solid solution and substantial ordering in the CaTs-rich part (Fig. 5). The disorder in the Di-rich part of the solution is slightly larger than that predicted by complete disorder of aluminum between the M1 and the tetrahedral site, perhaps suggesting some disorder of calcium between the M2 and the M1 site.

For the Gr–Py solid solution, excess enthalpies do not agree with the heats of solution measurements of Newton et al. (1977). While the heats of solution predict slightly asymmetric positive excess enthalpies with the maximum around $Gr_{30}Py_{70}$, the model gives the opposite asymmetry; slightly negative excess enthalpies for the Py-rich part of the solution and large positive excess enthalpies

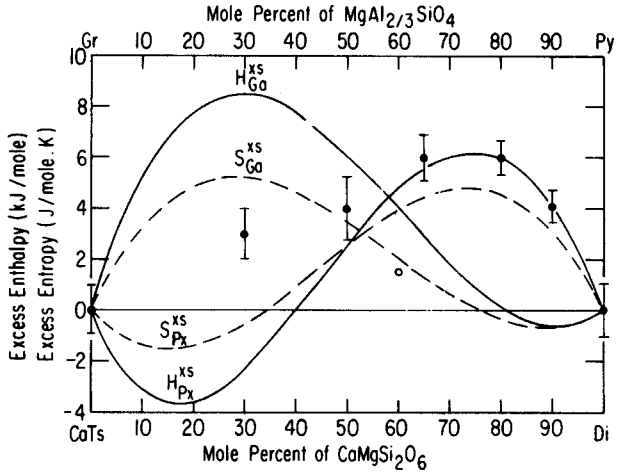

Fig. 5. Excess enthalpies and entropies of Di–CaTs and Gr–Py solid solutions. Solid dots represent excess enthalpies of clinopyroxene calculated from the heats of solution measurements of Newton et al. (1977). Open circle is the excess entropy of $Gr_{40}Py_{60}$ measured by Haselton (1979); the size of the symbol is comparable to the uncertainty of measurement.

for the Gr-rich part, with the maximum around $Gr_{70}Py_{30}$ (Fig. 5). It should be noted, however, that the model excess enthalpies of the Gr–Py solution are very similar to excess enthalpies of the grossular–almandine solution derived from phase equilibria by Cressey (1981) or obtained from heats of solution measurements by C. Geiger (personal communication). It is conceivable that the Py-rich compositions synthesized by Newton et al. from glass were metastably disordered. Geiger used substantially longer synthesis times, 24 hours vs. 3 hours. Ca-rich compositions could be unstable and decompose in the calorimeter producing pyroxene with a significantly more negative enthalpy of solution.

Excess entropies mimic the excess enthalpies, being slightly negative in the Py-rich part of the solution and largely positive in the Gr-rich part, with the maximum around $Gr_{70}Py_{30}$. For the composition $Gr_{40}Py_{60}$, the model gives 6 J/mol · K of excess entropy in reasonable agreement with 4.5 J/mol · K measured by Haselton (1979). Model excess entropies of the Gr–Py garnets are strikingly similar to the excess entropies of the grossular–almandine garnets reported by Cressey (1981).

The inferred mixing properties of the Gr–Py garnets, however, are not applicable to Py-rich garnets with compositions in the range Py_{100}–$Gr_{20}Py_{80}$. Garnet-bearing, two-pyroxene equilibria in the CMAS system indicate that for the Py-rich garnet containing 15 mol% of grossular the activity coefficient of pyrope is 1.040 at 1000°C and 1.007 at 1400°C (Gasparik, 1984). This translates to a positive excess enthalpy and entropy for the

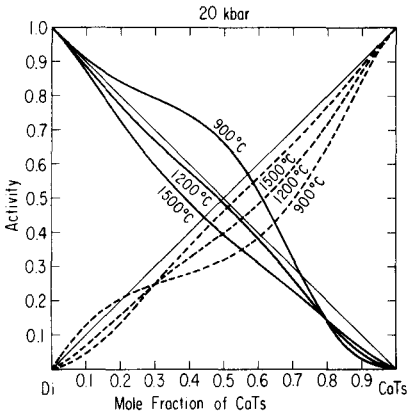

Fig. 6. Activity–composition relations for the Di–CaTs solid solution, calculated at 900, 1200 and 1500°C and 20 kbar. Solid lines—a_{Di}; dashed lines—a_{CaTs}.

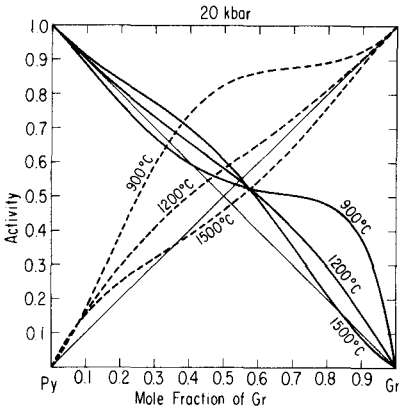

Fig. 7. Activity–composition relations for the Gr–Py solid solution, calculated at 900, 1200 and 1500°C and 20 kbar. Solid lines—a_{Py}; dashed lines—a_{Gr}.

garnet of this composition, in contrast to negative excess properties indicated by the model. If correct, the observations indicate a discontinuity in the mixing properties of the Py-rich garnets in the range $Gr_{15}Py_{85}$–$Gr_{20}Py_{80}$, most probably caused by ordering of the Ca and Mg cations in the dodecahedral site. The most likely candidate is the garnet of composition $Gr_{16.7}Py_{83.3}$ which has 1/6 or four of the dodecahedral sites in a unit cell occupied by calcium.

Activity–composition relations for Di–CaTs and Gr–Py solutions, calculated from the model, are shown in Figures 6 and 7 respectively. For much of the compositional range $a_{CaTs} < X_{CaTs}$ in contrast to Wood's (1979) conclusion that $a_{CaTs} \approx X_{CaTs}$.

Activities in the Gr–Py solution are almost always larger than the mole fractions. The model predicts unmixing at 828°C at 1 bar and 870°C at 20 kbar, with the crest of the garnet solvus at composition of $Gr_{70}Py_{30}$. The activity coefficient of grossular at 1200°C for $Gr_{20}Py_{80}$ composition is 1.47 which is in reasonable agreement with 1.40 calculated by Cressey (1981) from the phase equilibrium data of Hensen et al. (1975).

Phase relations in the join grossular–pyrope at 30 kbar

The melting relations in the join Gr–Py at 30 kbar by Malinovskii et al. (1976) and by Maaløe and Wyllie (1979) combined with the results of this study allow calculation of a complete phase diagram for the Gr–Py join. Although both previous studies attempted to present the subsolidus phase relations, the results are contradictory and mostly in disagreement with the present results. Unfortunately, there are also discrepancies between the two melting diagrams which cannot be resolved at present. Tentatively, the melting relations of Maaløe and Wyllie were adopted with modifications. All subsolidus phase boundaries shown in Figure 8 were calculated using the model described above.

The stability of Ga + Cpx is controlled by two equilibria:

$$3CaTs + 3Di = 2Gr + Py, \quad (7)$$

$$\Delta G°(7) = \Delta G°(1) + \Delta G°(3),$$

and

$$3CaTs + 3En = Gr + 2Py, \quad (8)$$

$$\Delta G°(8) = \Delta G°(1) + \Delta G°(2).$$

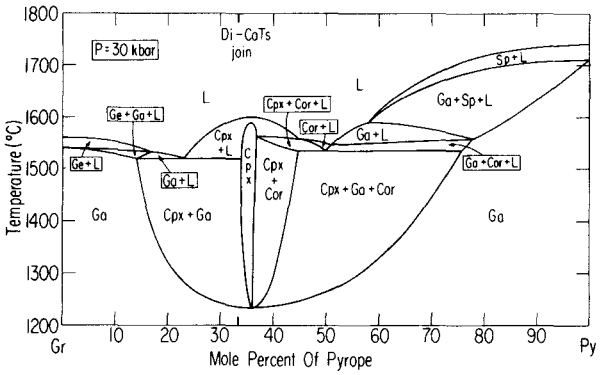

Fig. 8. *T–X* relations in the join Gr–Py at 30 kbar. The melting relations of Maaløe and Wyllie (1979) were modified to make them consistent with the presence of corundum. Incongruent melting of clinopyroxene has been adopted following Malinovskii et al. (1976). All subsolidus phase boundaries were calculated using the present model.

Stability of Cpx + Cor is controlled by:

$$2\text{Di} + 2\text{Cor} = 2\text{CaTs} + \text{En}, \quad (9)$$

$$\Delta G°(9) = 1/3[2\Delta G°(3) - 2\Delta G°(1) - \Delta G°(2)].$$

These reactions were used to calculate the boundaries of the clinopyroxene field, for which $X_{CaTs} = 0.5$.

In comparison with Figure 8, Maaløe and Wyllie failed to detect the narrowing of the solvus with decreasing temperature. They also ignored the presence of corundum. Malinovskii et al. show a field of Cpx + Cor but it is much narrower than the present calculations suggest it should be. Both studies show a wide stability field of clinopyroxene which extends far beyond the Di–CaTs join, suggesting the presence of the $CaSiO_3$ component in the pyroxene solution. If confirmed, this would mean that calcium can enter the M1 site in the pyroxene structure. The authors, however, do not present conclusive evidence and omit a discussion of this important observation.

There is very little evidence for the $CaSiO_3$ solubility in the Di–CaTs pyroxene. Boyd (1970) did not find excess $CaSiO_3$ in clinopyroxene coexisting with the Gr-rich garnet in four out of five experiments and expressed doubts about the one analysis which showed solid solution toward $CaSiO_3$. Kushiro (1964) and Davidson et al. (1979) found small excess of $CaSiO_3$ in synthetic diopsides but did not provide convincing evidence that this was not caused by wollastonite inclusions or intergrowths. Sekine and Wyllie (1983) reported 0.5 wt.% of excess $CaSiO_3$ in the synthesis run #341 at 1150°C/30 kbar but conceded that most of the clinopyroxenes in the run were metastable.

The present model does not allow for the excess of $CaSiO_3$ in clinopyroxene; all pyroxenes in the Gr–Py join have variable amounts of enstatite component. For the clinopyroxene coexisting with the Gr-rich garnet, the enstatite content decreases with increasing temperature from 3.7 mol% on the crest of the solvus to 0.7% on the solidus. In the presence of Py-rich garnet, the enstatite content on the solidus is 11.6%.

Acknowledgments

I am grateful to Robert C. Newton for valuable discussions and review of the manuscript. Reviews by S. R. Bohlen, C. T. Herzberg, and D. H. Lindsley are acknowledged. Research was supported by a National Science Foundation grant, EAR 81-07110 to R. C. Newton. Some conclusions are based on research conducted at the State University of New York at Stony Brook and supported by a National Science Foundation grant, EAR 80-26250 to D. H. Lindsley.

References

Birch, F. (1966) Compressibility; Elastic constants. In S. P. Clark, Ed., Handbook of Physical Constants, p. 97–173, Geological Society of America Memoir, 97, New York.

Boyd, F. R. (1970) Garnet peridotites and the system $CaSiO_3$–$MgSiO_3$–Al_2O_3. Mineralogical Society of America Special Paper, 3, 63–75.

Cameron, M. and Papike, J. J. (1980) Crystal chemistry of silicate pyroxenes. In C. T. Prewitt, Ed., Reviews in Mineralogy, vol. 7, Pyroxenes, p. 5–92. Mineralogical Society of America, Washington, D.C.

Charlu, T. V., Newton, R. C., and Kleppa, O. J. (1975) Enthalpies of formation at 970K of compounds in the system MgO–Al_2O_3–SiO_2 by high temperature solution calorimetry. Geochimica et Cosmochimica Acta, 39, 1487–1497.

Charlu, T. V., Newton, R. C., and Kleppa, O. J. (1978) Enthalpy of formation of some lime silicates by high-temperature solution calorimetry, with discussion of high pressure phase equilibria. Geochimica et Cosmochimica Acta, 42, 367–375.

Chatterjee, N. D. and Schreyer, W. (1972) The reaction enstatite$_{ss}$ + sillimanite = sapphirine$_{ss}$ + quartz in the system MgO–Al_2O_3–SiO_2. Contributions to Mineralogy and Petrology, 36, 49–62.

Chinner, G. A., Boyd, F. R., and England, J. L. (1960) Physical properties of garnet solid solutions. Carnegie Institute of Washington Year Book, 59, 76–78.

Cressey, G. (1981) Entropies and enthalpies of aluminosilicate garnets. Contributions to Mineralogy and Petrology, 76, 413–419.

Davidson, P. M., Engi, M., and Lindsley, D. H. (1979) The nature of clinopyroxene (cpx) solutions near Di($CaMgSi_2O_6$) in the system En–Wo ($Mg_2Si_2O_6$–$Ca_2Si_2O_6$), II (abstr.). Geological Society of America Abstracts with Programs, 11, 409.

Gasparik, T. (1981) Thermodynamic properties of pyroxenes in the NCMAS system saturated with silica. Ph.D. Thesis, State University of New York at Stony Brook.

Gasparik, T. (1984) Two-pyroxene thermobarometry with new experimental data in the system CaO–MgO–Al_2O_3–SiO_2. Contributions to Mineralogy and Petrology, 87, 87–97.

Gasparik, T. and Lindsley, D. H. (1980) Phase equilibria at high pressure of pyroxenes containing monovalent and trivalent ions. In C. T. Prewitt, Ed., Reviews in Mineralogy, vol. 7, Pyroxenes, p. 309–339. Mineralogical Society of America, Washington, D.C.

Gasparik, T. and Newton, R. C. (1984) The reversed alumina contents of orthopyroxene in equilibrium with spinel and forsterite in the system MgO–Al_2O_3–SiO_2. Contributions to Mineralogy and Petrology, 85, 186–196.

Grover, J. E. (1980) Thermodynamics of pyroxenes. In C. T. Prewitt, Ed., Reviews in Mineralogy, vol. 7, Pyroxenes, p. 341–417. Mineralogical Society of America, Washington, D.C.

Haselton, H. T. (1979) Calorimetry of synthetic pyrope–grossular garnets and calculated stability relations. Ph.D. Thesis, University of Chicago.

Haselton, H. T., Hemingway, B. S., and Robie, R. A. (1982) Low-temperature heat-capacity measurements on synthetic $CaAl_2SiO_6$ pyroxene (abstr.). EOS, Transactions, American Geophysical Union, 63, 467.

Haselton, H. T. and Newton, R. C. (1980) Thermodynamics of pyrope-grossular garnets and their stabilities at high temperatures and high pressures. Journal of Geophysical Research, 85, 6973–6982.

Hazen, R. M. and Finger, L. W. (1978) Crystal structures and compressibilities of pyrope and grossular to 60 kbar. American Mineralogist, 63, 297–303.

Hensen, B. J., Schmid, R., and Wood, B. J. (1975) Activity–composition relationships for pyrope–grossular garnet. Contri-

butions to Mineralogy and Petrology, 51, 161–166.

Holland, T. J. B. (1981) Thermodynamic analysis of simple mineral systems. In R. C. Newton, A. Navrotsky, and B. J. Wood, Eds., Advances in Physical Geochemistry, vol. 1, Thermodynamics of Minerals and Melts, p. 19–34. Springer-Verlag, New York.

Krupka, K. M., Kerrick, D. M., and Robie, R. A. (1979) Heat capacities of synthetic orthoenstatite and natural anthophyllite from 5 to 1000 K (abstr.). EOS, Transactions, American Geophysical Union, 60, 405.

Kushiro, I. (1964) The system diopside–forsterite–enstatite at 20 kilobars. Carnegie Institution of Washington Year Book, 63, 101–108.

Levien, K. and Prewitt, C. T. (1981) HIgh-pressure structural study of diopside. American Mineralogist, 66, 315–323.

Lindsley, D. H., Grover, J. E., and Davidson, P. M. (1981) The thermodynamics of the $Mg_2Si_2O_6$–$CaMgSi_2O_6$ join: a review and an improved model. In R. C. Newton, A. Navrotsky, and B. J. Wood, Eds., Advances in Physical Geochemistry, vol. 1, Thermodynamics of Minerals and Melts, p. 149–175. Springer-Verlag, New York.

Maaløe, S. and Wyllie, P. J. (1979) The join grossularite–pyrope at 30 kb and its petrological significance. American Journal of Science, 279, 288–301.

Malinovskii, I. Yu., Godovikov, A. A., Doroshev, A. M., and Ran, E. N. (1976) Silicate systems at high temperatures and pressures in connection with the petrology of the upper mantle and lower layers of the earth's crust. (in Russian) In A. A. Godovikov, Ed., Fizichesko-Khimicheskiye Uslovija Protsessov Mineraloobrazovaniya. . . ., p. 135–146. Akademia Nauk SSSR, Novosibirsk.

Newton, R. C., Charlu, T. V., and Kleppa, O. J. (1977) Thermochemistry of high pressure garnets and clinopyroxenes in the system CaO–MgO–Al_2O_3–SiO_2. Geochimica et Cosmochimica Acta, 41, 369–377.

Ralph, R. L. and Ghose, S. (1980) Enstatite, $Mg_2Si_2O_6$: compressibility and crystal structure at 21 kbar (abstr.). EOS, Transactions, American Geophysical Union, 61, 409.

Redlich, O. and Kister, A. T. (1948) Thermodynamics of nonelectrolyte solutions. Algebraic representation of thermodynamic properties and the classification of solutions. Industrial and Engineering Chemistry, 40, 345–348.

Robie, R. A., Hemingway, B. S., and Fisher, J. R. (1978) Thermodynamic properties of minerals and related substances at 298.15 K and 1 bar (10^5 Pascals) pressure and at higher temperatures. United States Geological Survey Bulletin, 1452, Washington, D.C.

Saxena, S. K. (1976) Entropy estimates for some silicates at 298°K from molar volumes. Science, 193, 1241–1242.

Sekine, T. and Wyllie, P. J. (1983) Phase relationships in the join grossularite–pyrope–7.5 percent H_2O at 30 kb. American Journal of Science, 283, 435–453.

Skinner, B. J. (1966) Thermal expansion. In S. P. Clark, Ed., Handbook of Physical Constants, p. 75–96. Geological Society of America Memoir, 97, New York.

Sobolev, N. V., Jr., Kuznetsova, I. K., and Zyuzin, N. I. (1968) The petrology of grospydite xenoliths from the Zagadochnaya kimberlite pipe in Yakutia. Journal of Petrology, 9, 253–280.

Wood, B. J. (1979) Activity–composition relationships in Ca(Mg, Fe)Si_2O_6–$CaAl_2SiO_6$ clinopyroxene solutions. American Journal of Science, 279, 854–875.

Manuscript received, January 2, 1984;
accepted for publication, June 27, 1984.

Appendix

The Redlich-Kister equation for excess free energy of a ternary solid solution has the following form (Redlich and Kister, 1948; Grover, 1980, p. 365):

$$G^{xs} = X_1X_2[A_{12} + B_{12}(X_1-X_2) + C_{12}(X_1-X_2)^2 + D_{12}(X_1-X_2)^3 + \ldots]$$
$$+ X_1X_3[A_{13} + B_{13}(X_1-X_3) + C_{13}(X_1-X_3)^2 + D_{13}(X_1-X_3)^3 + \ldots]$$
$$+ X_2X_3[A_{23} + B_{23}(X_2-X_3) + C_{23}(X_2-X_3)^2 + D_{23}(X_2-X_3)^3 + \ldots]$$
$$+ X_1X_2X_3[A + B_{2,1}(X_1-X_2) + B_{3,1}(X_1-X_3) + Z_1(X_2-X_3)].$$

The excess chemical potential of component "k" in a solid solution can be calculated using the following general expression (Grover, 1980, p. 413):

$$\mu_k^{xs} = RT\ln\gamma_k = G^{xs} - \sum_{i,i\neq k}^{c} X_i\left(\frac{\partial G^{xs}}{\partial X_i}\right)_{T,P,X_{j\neq k,i}}$$

Expressions for excess chemical potentials of all components in a ternary solid solution follow:

$$RT\ln\gamma_1 = A_{12}(X_2^2+X_2X_3) + B_{12}(3X_2^2-4X_2^3+2X_2X_3-6X_2^2X_3-2X_2X_3^2)$$
$$+ C_{12}(12X_2^4-16X_2^3+5X_2^2+3X_2X_3-20X_2^2X_3+15X_2^2X_3^2-6X_2X_3^2+24X_2^3X_3+3X_2X_3^3)$$
$$+ A_{13}(X_3^2+X_2X_3) + B_{13}(3X_3^2-4X_3^3+2X_2X_3-2X_2^2X_3-6X_2X_3^2)$$
$$+ C_{13}(12X_3^4-16X_3^3+5X_3^2+3X_2X_3-6X_2^2X_3+15X_2^2X_3^2-20X_2X_3^2+3X_2^2X_3+24X_2X_3^3)$$
$$+ A_{23}(-X_2X_3) + B_{23}(2X_2X_3^2-2X_2^2X_3) + C_{23}(6X_2^2X_3^2-3X_2^2X_3-3X_2X_3^2) + \ldots$$

$$RT\ln\gamma_2 = A_{12}(X_1^2+X_1X_3) + B_{12}(4X_1^3-3X_1^2-2X_1X_3+6X_1^2X_3+2X_1X_3^2)$$
$$+ C_{12}(12X_1^4-16X_1^3+5X_1^2+3X_1X_3-20X_1^2X_3+15X_1^2X_3^2-6X_1X_3^2+24X_1^3X_3+3X_1X_3^3)$$
$$+ A_{13}(-X_1X_3) + B_{13}(2X_1X_3^2-2X_1^2X_3) + C_{13}(6X_1^2X_3^2-3X_1^2X_3-3X_1X_3^2)$$
$$+ A_{23}(X_3^2+X_1X_3) + B_{23}(3X_3^2-4X_3^3+2X_1X_3-2X_1^2X_3-6X_1X_3^2)$$
$$+ C_{23}(12X_3^4-16X_3^3+5X_3^2+3X_1X_3-6X_1^2X_3+15X_1^2X_3^2-20X_1X_3^2+3X_1^2X_3+24X_1X_3^3) + \ldots$$

$$RT\ln\gamma_3 = A_{12}(-X_1X_2) + B_{12}(2X_1X_2^2-2X_1^2X_2) + C_{12}(6X_1^2X_2^2-3X_1^2X_2-3X_1X_2^2)$$
$$+ A_{13}(X_1^2+X_1X_2) + B_{13}(4X_1^3-3X_1^2-2X_1X_2+6X_1^2X_2+2X_1X_2^2)$$
$$+ C_{13}(12X_1^4-16X_1^3+5X_1^2+3X_1X_2-20X_1^2X_2+15X_1^2X_2^2-6X_1X_2^2+24X_1^2X_2+3X_1X_2^2)$$
$$+ A_{23}(X_2^2+X_1X_2) + B_{23}(4X_2^3-3X_2^2-2X_1X_2+2X_1^2X_2+6X_1X_2^2)$$
$$+ C_{23}(12X_2^4-16X_2^3+5X_2^2+3X_1X_2-6X_1^2X_2+15X_1^2X_2^2-20X_1X_2^2+3X_1^2X_2+24X_1X_2^3) + \ldots$$

The temperature and pressure dependence of the parameters was expressed in a familiar form, e.g.:

$$A_{12} = A_{G,12} = A_{H,12} - TA_{S,12} + PA_{V,12}, \text{ etc.}$$

The Redlich-Kister parameters can be compared with the more frequently used Margules parameters of an asymmetric subregular solid solution by using the following simple relations:

$$W_{12} = A_{12} - B_{12},$$
$$W_{21} = A_{12} + B_{12}, \text{ etc.}$$